



Tetrakis(phthalocyaninato) terbium–cadmium quadruple-decker liquid crystals with good semiconducting properties

Qi Ma^a, Hailong Wang^a, Yanli Chen^{b,*}, Jianzhuang Jiang^{a,*}

^a Beijing Key Laboratory for Science and Application of Functional Molecular and Crystalline Materials, Department of Chemistry, University of Science and Technology Beijing, Beijing 100083, China

^b Shandong Provincial Key Laboratory of Fluorine Chemistry and Chemical Materials, School of Chemistry and Chemical Engineering, University of Jinan, Jinan 250022, China

ARTICLE INFO

Article history:

Received 26 March 2014

Received in revised form 16 July 2014

Accepted 24 July 2014

Available online 6 August 2014

Keywords:

Phthalocyanine

Quadruple-decker

Ionic liquid crystal

Electric conductivity

ABSTRACT

Neutral and mono-oxidized states of novel sandwich-type tetrakis[2,3,9,10,16,17,23,24-octa(dodecanoyloxy)phthalocyaninato] terbium–cadmium quadruple-decker complex $\{[\text{Pc}(\text{OC}_{12}\text{H}_{25})_8]\text{Tb}[\text{Pc}(\text{OC}_{12}\text{H}_{25})_8]\text{Cd}[\text{Pc}(\text{OC}_{12}\text{H}_{25})_8]\text{Tb}[\text{Pc}(\text{OC}_{12}\text{H}_{25})_8]\}$ (**1**) and $\{[\text{Pc}(\text{OC}_{12}\text{H}_{25})_8]\text{Tb}[\text{Pc}(\text{OC}_{12}\text{H}_{25})_8]\text{Cd}[\text{Pc}(\text{OC}_{12}\text{H}_{25})_8]\text{Tb}[\text{Pc}(\text{OC}_{12}\text{H}_{25})_8]\}$ - SbCl_6 (**2**) were synthesized and spectroscopically characterized. Polarized optical microscope (POM) together with differential scanning calorimeter (DSC) measurement revealed their similar two rectangular columnar mesophases over a relatively lower temperature range and higher temperature range, respectively, within their wide liquid crystal temperature range of 19–266 °C for **1** and 4–249 °C for **2**. Temperature-dependent X-ray diffraction (XRD) analysis result disclosed the slight difference in terms of the neighboring quadruple-decker π – π stacking between these two mesophases, which in turn accounts for their electric conducting behavior along with the change in temperature. In addition, due to the ionic conductive nature, the mono-oxidized liquid crystals of **2** display more than 2 order of magnitude higher electric conductivity than that for **1**, with the highest value $4.1 \times 10^{-4} \text{ S cm}^{-1}$ achieved at 140 °C.

© 2014 Elsevier B.V. All rights reserved.

1. Introduction

Liquid crystals (LCs), as an important self-organized functional soft materials, have found a wide range of applications such as liquid–crystal display technology, single-molecule magnets, and biomaterials [1]. In recent years, the aromatic core-based liquid crystals, which are also known as discotic liquid crystals, have received increasing research interest due to their good semiconductivity in the mesophase associated with effective π – π intermolecular

stacking among their self-organized liquid crystal molecules [2]. As one of the most important functional molecular materials with large π -conjugated electronic structure and extraordinary thermal and photochemical stability [3], phthalocyanine derivatives have been among the most intensively studied discotic liquid crystal materials due to their strong absorption in the visible and NIR regions, which enables their applications in optoelectronic devices [4].

Monomeric phthalocyanine derivatives with discotic liquid crystal behavior were first reported in 1982 [5]. In the following years, more extensive studies have been carried out in this direction, leading to the report of a large number of various phthalocyanine liquid crystals with

* Corresponding authors. Tel.: +86 (0)531 8973 6150 (Y. Chen). Tel.: +86 (0)10 6233 2592; fax: +86 (0)10 6233 2462 (J. Jiang).

E-mail addresses: chm_chenyl@ujn.edu.cn (Y. Chen), jianzhuang@ustb.edu.cn (J. Jiang).

good stability and electric conductivity [6]. Due also to the good semiconducting properties revealed for the sandwich-type bis(phthalocyaninato) rare earth complexes, the phase behaviors of quite a number of such kind of double-deckers have been systematically studied for potential applications in various organic electronic devices [7]. Quite recently, the mesophase behavior of tris(phthalocyaninato) rare earth complexes was also investigated by this group [8]. However, despite the quite systematic studies of the semiconducting properties of both monomeric phthalocyanine and bis(phthalocyaninato) rare earth liquid crystals, the electric conductivity for the liquid crystals based on the tris(phthalocyaninato) rare earth triple-decker or sandwiches with more than three phthalocyanine decks has not yet been reported thus far.

Very recently, novel sandwich-type tetrakis(phthalocyaninato) rare earth-cadmium quadruple-decker complexes were synthesized on the basis of the capability of phthalocyanine to coordinate with divalent transition metal of cadmium in the formation of stacked tetrapyrrole metal oligomers. The tetrapyrrole rare earth-cadmium quadruple-decker analogs have aroused increasing attention because of the extension of the π networks along the axis perpendicular to the macrocycle plane, which makes them even more promising as active materials for efficient charge transport compared with their double-/triple-decker counterparts [9]. For the purpose of introducing the mesophase behavior into this new species of sandwich compounds with large fraction of aromatic discotic core, long dodecanoyloxy chains were incorporated onto the phthalocyanine periphery in the quadruple-decker molecule, yielding tetrakis[2,3,9,10,16,17,23,24-octa(dodecanoyloxy)phthalocyaninato] terbium-cadmium quadruple-decker complex $\{[\text{Pc}(\text{OC}_{12}\text{H}_{25})_8]\text{Tb}[\text{Pc}(\text{OC}_{12}\text{H}_{25})_8]\text{Cd}[\text{Pc}(\text{OC}_{12}\text{H}_{25})_8]\text{Tb}[\text{Pc}(\text{OC}_{12}\text{H}_{25})_8]\}$ (**1**), [Scheme 1](#). Oxidation with phenoxathiin hexachloroantimonate afforded the mono-oxidized derivative $\{[\text{Pc}(\text{OC}_{12}\text{H}_{25})_8]\text{Tb}[\text{Pc}(\text{OC}_{12}\text{H}_{25})_8]\text{Cd}[\text{Pc}(\text{OC}_{12}\text{H}_{25})_8]\text{Tb}[\text{Pc}(\text{OC}_{12}\text{H}_{25})_8]\}$ · SbCl_6 (**2**). Both neutral and mono-oxidized states exhibited two similar rectangular columnar LC mesophases within their wide liquid crystal temperature range from 19 to 266 °C for **1** and 4 to 249 °C for **2**, respectively, with slight differences in terms of the neighboring quadruple-decker π - π stacking between these two mesophases. This in turn rationalizes their electric conducting behavior as a function of temperature. In addition, due to the ionic conductive nature [10], the mono-oxidized liquid crystals of **2**

display more than 2 order of magnitude higher electric conductivity than that for **1**, with the highest value $4.1 \times 10^{-4} \text{ S cm}^{-1}$ achieved at 140 °C.

2. Experimental section

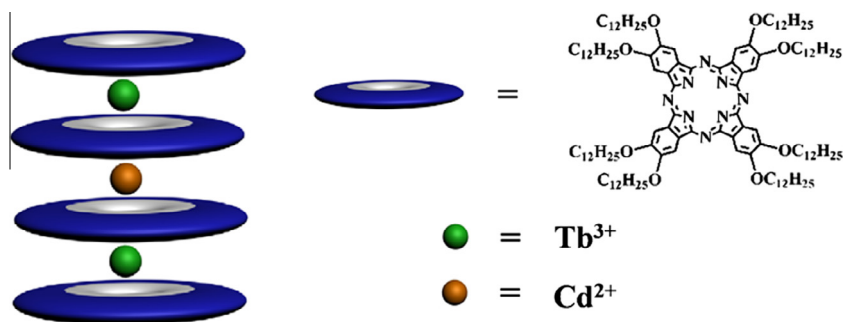
2.1. General remarks

All the reagents and solvents were used as received. The compounds of $\{[\text{Pc}(\text{OC}_{12}\text{H}_{25})_8]\text{Tb}[\text{Pc}(\text{OC}_{12}\text{H}_{25})_8]\}$ [11] and phenoxathiin hexachloroantimonate [12] were prepared according to published procedure.

Electronic absorption spectra were recorded on a PerkinElmer Lambda 750 UV/VIS Spectrophotometer. MALDI-TOF mass spectra were taken on a Bruker BIFLEX III ultra-high-resolution Fourier-transform ion-cyclotron-resonance (FT-ICR) mass spectrometer with alpha-cyano-4-hydroxycinnamic acid as matrix. Elemental analysis was performed on an Elementar Vavio El III. Phase transition behavior was observed using a Carl Zeiss Axio Cscope. A1 polarized optical microscope (POM) with a Linkam LTS420 liquid crystal freezing and heating stage system. Differential scanning calorimeter (DSC) measurements were performed on a Perkin Elmer DSC8000. The X-ray diffraction measurements were carried out using Rigaku D-Max (Cu $K\alpha$ radiation) equipped with a heating plate controlled by a thermoregulator.

2.2. Synthesis of $\{[\text{Pc}(\text{OC}_{12}\text{H}_{25})_8]\text{Tb}[\text{Pc}(\text{OC}_{12}\text{H}_{25})_8]\text{Cd}[\text{Pc}(\text{OC}_{12}\text{H}_{25})_8]\text{Tb}[\text{Pc}(\text{OC}_{12}\text{H}_{25})_8]\}$ (**1**)

A mixture of $\text{Cd}(\text{OAc})_2 \cdot 2\text{H}_2\text{O}$ (5.3 mg, 0.02 mmol) and neutral bis(phthalocyaninato) terbium double-decker $\{[\text{Pc}(\text{OC}_{12}\text{H}_{25})_8]\text{Tb}[\text{Pc}(\text{OC}_{12}\text{H}_{25})_8]\}$ (42.5 mg, 0.01 mmol) in 1,2,4-trichlorobenzene (TCB) (4 mL) was heated to reflux under nitrogen for 2.5 h. After being cooled to room temperature, the volatiles were removed under reduced pressure. The residue was chromatographed on a silica gel column using CHCl_3 as the eluent to give a green band, which contained mainly the unreacted $\{[\text{Pc}(\text{OC}_{12}\text{H}_{25})_8]\text{Tb}[\text{Pc}(\text{OC}_{12}\text{H}_{25})_8]\}$. Further elution with CHCl_3 gave a blue band containing the target quadruple-decker complex $\{[\text{Pc}(\text{OC}_{12}\text{H}_{25})_8]\text{Tb}[\text{Pc}(\text{OC}_{12}\text{H}_{25})_8]\text{Cd}[\text{Pc}(\text{OC}_{12}\text{H}_{25})_8]\text{Tb}[\text{Pc}(\text{OC}_{12}\text{H}_{25})_8]\}$ (**1**). Repeated chromatography gave the pure homoleptic quadruple-decker complex **1** in the yield of 18.1 mg, 43%.



Scheme 1. Schematic molecular structure of tetrakis(phthalocyaninato) Tb(III)-Cd(II) quadruple-decker complex.

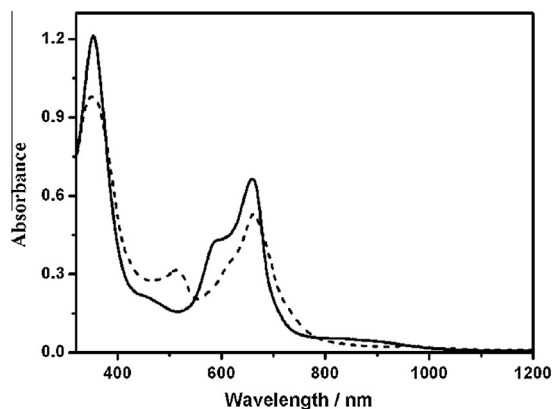


Fig. 1. Electronic absorption spectra of **1** (solid line) and **2** (dash line) at the concentration of 5×10^{-6} M in CH_2Cl_2 .

2.3. Synthesis of $\{[\text{Pc}(\text{OC}_{12}\text{H}_{25})_8]\text{Tb}[\text{Pc}(\text{OC}_{12}\text{H}_{25})_8]\text{Cd}[\text{Pc}(\text{OC}_{12}\text{H}_{25})_8]\text{Tb}[\text{Pc}(\text{OC}_{12}\text{H}_{25})_8]\} \cdot \text{SbCl}_6$ (**2**)

Phenoxathiin hexachloroantimonate (3.2 mg, 0.006 mmol) was added into a solution of **1** (50.0 mg, 0.006 mmol) dissolved in 200 mL CH_2Cl_2 at room temperature under a nitrogen atmosphere [13]. The solution was stirred for 30 min as monitored by UV–vis spectroscopy.

3. Result and discussion

3.1. Synthesis and characterization

Following the published procedure [9], homoleptic tetrakis[2,3,9,10,16,17,23,24-octa(dodecanoyloxy)phthalocyaninato] terbium–cadmium quadruple-decker complex $\{[\text{Pc}(\text{OC}_{12}\text{H}_{25})_8]\text{Tb}[\text{Pc}(\text{OC}_{12}\text{H}_{25})_8]\text{Cd}[\text{Pc}(\text{OC}_{12}\text{H}_{25})_8]\text{Tb}[\text{Pc}(\text{OC}_{12}\text{H}_{25})_8]\}$ (**1**) was prepared in relatively good yield with the neutral unprotonated bis(phthalocyaninato) terbium double-decker as starting material in the presence of cadmium acetate in refluxing TCB. Oxidation of this quadruple-decker compound by phenoxathiin hexachloroantimonate provided the mono-oxidized quadruple-decker species $\{[\text{Pc}(\text{OC}_{12}\text{H}_{25})_8]\text{Tb}[\text{Pc}(\text{OC}_{12}\text{H}_{25})_8]\text{Cd}[\text{Pc}(\text{OC}_{12}\text{H}_{25})_8]\text{Tb}[\text{Pc}(\text{OC}_{12}\text{H}_{25})_8]\} \cdot \text{SbCl}_6$ (**2**) in almost the quantitative yield. Satisfactory elemental analysis results were obtained for both the newly prepared quadruple-decker complexes **1** and **2**.

The MALDI-TOF mass spectra of both compounds clearly showed intense signal for corresponding molecular ion $[\text{M}]^+$, Table S1 (Supplementary material), indicating their sandwich quadruple-decker nature with the composition of two terbium cations, one cadmium cation, and four phthalocyanine ligands.

3.2. Electronic absorption spectra

The electronic absorption spectra of both the neutral and mono-oxidized quadruple-deckers **1** and **2** were recorded in CH_2Cl_2 and are compared in Fig. 1. The absorption for **1** at 352 nm is attributed to the phthalocyanine Soret band for the neutral quadruple-decker, while the one at 659 nm with a shoulder at 587 nm to the phthalocyanine Q-band. As can be seen in Fig. 1, after oxidizing the neutral species **1** into the mono-oxidized analog **2**, both the Soret absorption and the main Q band of phthalocyanine are almost unchanged at 351 and 661 nm. However, the shoulder Q band at 587 nm for **2** disappears, while a new absorption with low intensity appears at 514 nm associated with the phthalocyanine π -radical due to the transition from the deep occupied molecular orbitals to the semi-occupied HOMO [14]. It is worth mentioning that the whole oxidation procedure of **1** with phenoxathiin hexachloroantimonate was monitored by UV–vis spectroscopy and is shown in Fig. S1 (Supplementary material) for the readers convenience.

The electronic absorption spectra of solution-cast films of these two quadruple-decker complexes at room temperature on the quartz substrate were also recorded and given in Figs. S2 and S3 (Supplementary material), respectively. As shown in Fig. S2 (Supplementary material), when dispersed on the quartz substrate, both the phthalocyanine Soret and Q bands for **1** significantly blue shift from 352, 659, and 587 nm in CH_2Cl_2 to 343, 651, and 567 nm, respectively. This is also true for the mono-oxidized compound **2** with the Soret band blue-shifted into the region far less than 300 nm and the Q absorptions from 661 and 514 nm in solution to 489 and 378 nm on the quartz substrate, Fig. S3 (Supplementary material). The mono-oxidized complex shows a much larger blue shift from solution to film than the neutral complex due likely to the strong electrostatic interactions between mono-oxidized complex and its counterparts in the solid state. On the basis of Kasha's excitation theory [15], blue shift in the

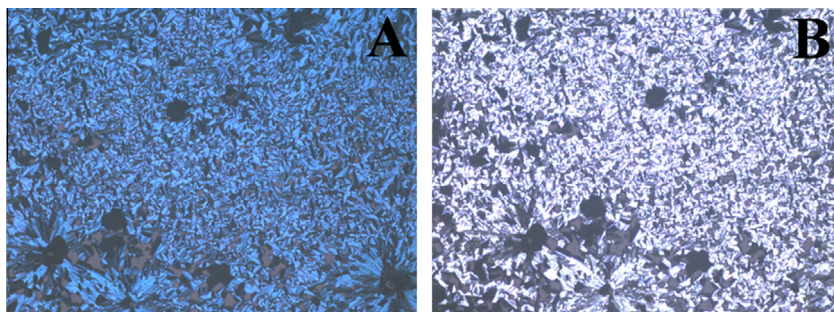


Fig. 2. The POM textures (200 \times magnification) of **1** at 250 (A) and 130 (B) $^\circ\text{C}$.

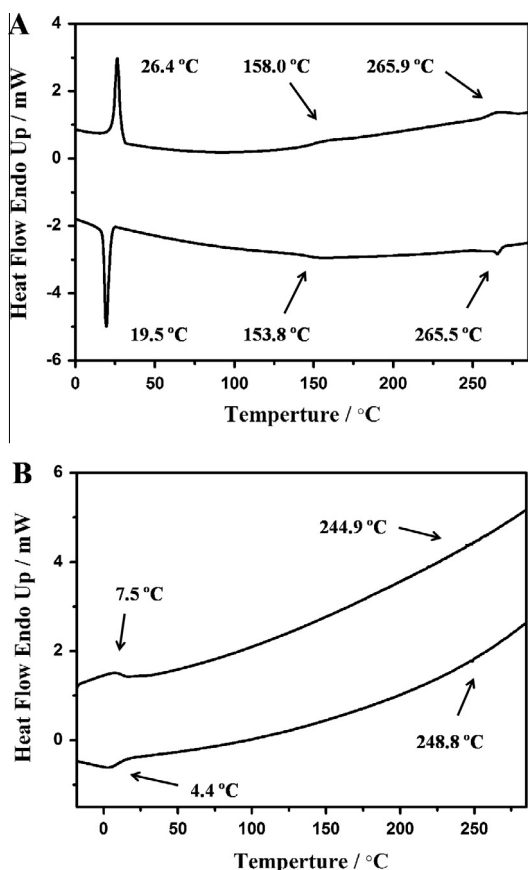


Fig. 3. DSC thermograms of **1** (A) and **2** (B) on second heating/cooling at 10 °C/min (the upper line is heating and the lower line is cooling).

main absorption bands of both **1** and **2** upon aggregation is typically a sign of the effective π - π interaction between neighboring molecules of both neutral and mono-oxidized states, indicating the formation of *H*-aggregate for both compounds on the quartz substrate at room temperature (actually in the liquid crystal state). This result is in good accordance with the XRD analysis as detailed below.

3.3. Mesogenic properties

The liquid crystal phase transition behavior of both **1** and **2** was first observed by polarizing optical microscope (POM) in the range of 25–300 °C for samples placed between a clean untreated glass slide and a cover slip. As shown in Fig. 2A, upon cooling from isotropic liquid to 250 °C at a rate of 10 °C/min, the neutral quadruple-decker compound **1** displays a fan-shaped dendritic texture, typical of columnar mesophase [16]. Continuous decrease in the temperature to 130 °C does not induce any noticeable change in the liquid crystal dendritic texture. However, the color changed from blue for the liquid crystal at 250 °C to purple for the one at 130 °C, Fig. 2B, suggesting the change in the columnar mesophase of **1** occurring in this temperature range between 250 and 130 °C. This is indeed verified by the DSC as well as the X-ray diffraction analysis result as detailed below. Further cooling until

room temperature leads to no noticeable change in both the dendritic texture and color of the mesophase, Fig. S4 (Supplementary material), indicating the liquid crystal state of **1** even at room temperature. This actually is also true for the mono-oxidized quadruple-decker species **2**, Fig. S5 (Supplementary material), with the change in the isotropic transition temperature appearing at 249 °C.

The phase transition temperatures for the quadruple-decker compounds were further measured by differential scanning calorimeter (DSC) in the range of 0–280 °C. As summarized in Table S2 (Supplementary material) and shown in Fig. 3A, for the neutral quadruple-decker **1**, three distinct endothermic peaks around 26.4, 158.0, and 265.9 °C were observed in the DSC thermogram, corresponding to the phase transition from crystalline to columnar mesophase, from columnar mesophase to isotropic liquid, respectively. Upon cooling from 280 to 0 °C, the same three transitions are mirrored with hysteresis at about 19.5, 153.8, and 265.5 °C. Obviously, observation of the phase transition by DSC for the liquid crystal of **1** at about 153.8 °C is in good agreement with the above mentioned POM result. As for the mono-oxidized species **2**, despite the feasible columnar mesophase transition suggested by the POM technique, a corresponding endothermic peak was not observed in the temperature range between 250 and 130 °C in the DSC thermogram, Fig. 3B. The only two endothermic peaks observed at around 7.5 and 244.9 °C upon heating and at about 4.4 and 248.8 °C upon cooling in the DSC thermograms correspond to the phase transition from crystalline to columnar mesophase and from columnar mesophase to isotropic liquid, respectively.

The molecular packing of the compounds in liquid crystal phases was examined by temperature-dependent X-ray diffraction analysis. Fig. 4 shows the XRD diffraction patterns of **1** at different temperatures. It is worth noting that for the purpose of differentiating the mesophase of **1** between ca. 160 and 260 °C from that at relatively lower temperature range by XRD method, the sample was held above its clear point temperature for 20 min and then cooled to 200 °C. As shown in the XRD pattern recorded at this temperature, Fig. 4, three peaks were revealed in the low angle range at ca. 28.9 Å ($2\theta = 3.1^\circ$), 17.2 Å

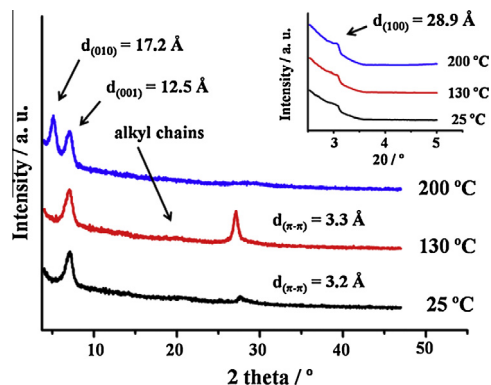


Fig. 4. XRD diffraction patterns of the mesophase of **1** at different temperatures.

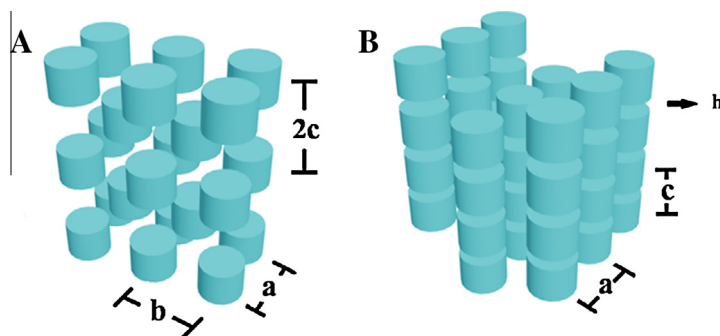


Fig. 5. Schematic molecular packing in the columnar liquid mesophases Col_{r1} (A) and Col_{r2} (B) formed from **1**, respectively.

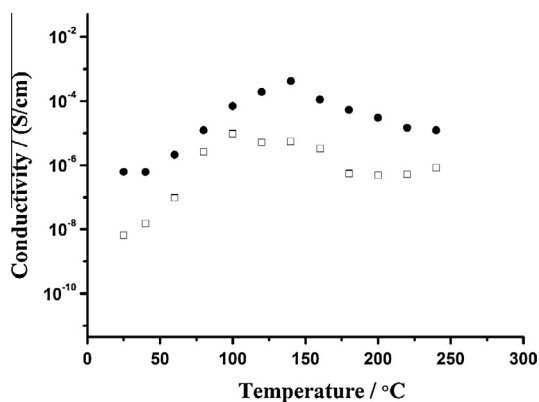


Fig. 6. *I*–*V* curves measured on the liquid crystal materials formed from **1** (□) and **2** (●), respectively, as a function of temperature.

($2\theta = 5.1^\circ$), and *ca.* 12.5 Å ($2\theta = 7.1^\circ$), originating from the (100), (010), and (001) planes, respectively. The former two peaks are related with the distance between the neighboring columns in two different directions and the latter one with the distance between the centers of two neighboring quadruple-decker molecules within the column of the rectangular columnar (Col_{r1}) mesophase. These diffraction results could be assigned to the reflections from a rectangular lattice with the cell parameter of $a = 28.9$ Å, $b = 17.2$ Å, and $c = 12.5$ Å, Fig. 5. Upon being cooled to 130 °C, along with the change in the mesophase to the one at relatively lower temperature range between *ca.* 19 and 160 °C as detailed above by POM and DSC measurement, significant change occurs in the XRD diffraction pattern, Fig. 4.

In the low angle region, the peak originating from the (010) plane due to the distance between the neighboring columns along the *b* axis disappears, indicating the loss of molecular ordering along this direction. While the other two peaks that originate from the (100) and (001) planes are almost unchanged in the XRD pattern, indicating the appearance of a new rectangular columnar (Col_{r2}) mesophase with the lattice parameters of $a = 28.9$ Å ($2\theta = 3.1^\circ$) and $c = 12.5$ Å ($2\theta = 7.1^\circ$). In the wide angle region, a new sharp diffraction peak was observed at 3.3 Å ($2\theta = 27.1^\circ$), denoted as *h*, and is due to the average π – π distance between the quadruple-decker molecules [9,17], Fig. 5. It

is noteworthy that the loss of regular molecular ordering between the 2D *ac* layers along the *b*-axis due to the unfavorable mixing among the rigid Pc core and flexible side chains seems to correspond well with the simultaneous stacking up of π -conjugated cores along the *h* direction for the liquid crystal at this temperature range in terms of the energy balance. Further cooling from 130 °C till room temperature does not result in significant change in the X-ray diffraction pattern except the very slight shift in the position of the peak due to the average π – π distance, which indicates the very slight change in the π – π stacking from 3.3 to 3.2 Å, Fig. 4. In addition, as can be clearly seen from Fig. 4, along with the decrease in temperature, the relatively broad halo due to the molten alkyl chains at *ca.* 4.3 Å ($2\theta = 20.5^\circ$) gets a bit of more obvious. This is also true in particular for the case of **2**, Fig. S6 (Supplementary material).

X-ray diffraction analysis over the liquid crystal mesophases of the mono-oxidized compound **2** at different temperatures, Fig. S6 (Supplementary material), actually revealed its very much similar liquid crystal mesophases with similar molecular packing to **1**. In line with the POM experimental result, two rectangular columnar (Col_r) mesophase states have been disclosed between the isotropic and crystalline phase of **2** by the temperature-dependent X-ray diffraction analysis result. On the basis of the XRD pattern recorded at 200 °C for **2**, a rectangular columnar (Col_{r1}) mesophase existing at higher temperature range with the cell parameters $a = 28.8$ Å ($2\theta = 3.0^\circ$), $b = 18.4$ Å ($2\theta = 4.8^\circ$), and $c = 12.6$ Å ($2\theta = 7.1^\circ$), respectively, Fig. S6 (Supplementary material), and a similar one (Col_{r2}) existing at relatively lower temperature range with the lattice parameters of 28.8 Å ($2\theta = 3.0^\circ$) and $c = 12.6$ Å ($2\theta = 7.1^\circ$) could be deduced.

3.4. *I*–*V* properties

To demonstrate the potential application of the liquid crystal materials formed from homoleptic tetrakis[2,3,9,10,16,17,23,24-octa(dodecanoyloxy)phthalocyaninato] terbium–cadmium quadruple-decker compounds in electronic devices, Au electrodes were thermally evaporated onto the liquid crystal structures to measure their current–voltage characteristics. The conductivity, σ , can be calculated by the following equation [18]: $\sigma = d \times I /$

$[(2n - 1) \times L \times h \times V]$, where d is the inter-electrode spacing, I the current, n the number of electrode digits, L the overlapping length of the electrodes, h the calculated thickness of the aggregates, and V the voltage.

Fig. 6 shows the conductivity estimated from current–voltage (I – V) characteristics of liquid crystal materials formed from **1** and **2** as a function of temperature. As can be seen, over the same liquid crystal temperature range, the mono-oxidized quadruple-decker **2** shows much higher electric conductivity in the range of 6.2×10^{-7} – 4.1×10^{-4} S cm⁻¹ than that of the neutral analog **1**, 6.6×10^{-9} – 5.4×10^{-6} S cm⁻¹ due to the ionic conductive nature of the former compound. The liquid crystal material of **1** formed at room temperature exhibits the lowest conductivity of 6.6×10^{-9} S cm⁻¹ due to the less molecular ordering. With increasing temperature, the conductivity obtained for the liquid crystals of this compound increases in the same trend of compound **2** with the highest value of 9.5×10^{-6} S cm⁻¹ achieved at the phase transition temperature around 160 °C, which then gets decreased along with the further increase in the temperature, Fig. 6. Interestingly, this result seems to be in good agreement with the molecular ordering degree as suggested by the XRD analysis. As indicated above, the molecular ordering in particular in terms of the intermolecular π – π stacking in the mesophase of **1** is gradually enhanced along with the increase in temperature, with the highest degree achieved also at the phase transition temperature at 160 °C, after which ordering diminishes with further increase in temperature. As a consequence, intermolecular π – π stacking between neighboring quadruple-decker molecules within the column in the rectangular columnar mesophase is responsible for the semiconducting properties of the sandwich tetrakis(phthalocyaninato) terbium–cadmium quadruple-decker liquid crystals. In particular, this is also true for the mono-oxidized analog despite the ionic conductive nature of this complex. The good semiconducting properties unveiled for the liquid crystal film of novel sandwich-type tetrakis(phthalocyaninato) rare earth quadruple-decker complex in particular in the mono-oxidized state at relatively high temperature indicate their potential application in solution-processable organic electronics. It is worth noting that, in comparison with the DC conductivities of double-decker liquid crystals such as bis[tetrakis(alkylthio)phthalocyaninato]lutetium(III) double-decker complexes Lu₂[(C_{*n*}H_{2*n*+1S})₄Pc]₂ ($n = 10, 12, 16$) in the range of 10^{-7} to 10^{-8} S/cm [19], the quadruple-deckers in the present case have shown higher conductivity due to the extended π networks along the axis perpendicular to the macrocycle plane. However, these quadruple-decker liquid crystals are less conductive than the triple-decker Eu₂[Pc(15C5)₄]₂[Pc(OC₁₀H₂₁)₈] according to our previous study [18] due probably to the increase in the hopping distance between the neighboring hopping centers associated with the increase in the alkyl chain length in the quadruple-decker liquid crystals [20].

4. Conclusions

Novel sandwich-type tetrakis[2,3,9,10,16,17,23,24-octa(dodecanoyloxy)phthalocyaninato] terbium–cadmium

quadruple-decker complex in both neutral and mono-oxidized states was revealed to exhibit two rectangular columnar mesophases within a relatively wide liquid crystal temperature range. The slight difference in terms of the neighboring quadruple-decker π – π stacking between these two mesophases accounts well for their electric conducting behavior along with the change in temperature. However, the mono-oxidized liquid crystals of **2** display more than 2 order of magnitude higher electric conductivity than that for **1** due to the ionic conductive nature. The highest electric conductivity, 4.1×10^{-4} S cm⁻¹, achieved for the mesophase of **2** at 140 °C reveals its great potential applications in various organic nano-electronics.

Acknowledgments

Financial support from the National Key Basic Research Program of China (Grant Nos. 2013CB933402 and 2012CB224801), Natural Science Foundation of China, Beijing Municipal Commission of Education, and University of Science and Technology Beijing, is gratefully acknowledged.

Appendix A. Supplementary material

Supplementary data associated with this article can be found, in the online version, at <http://dx.doi.org/10.1016/j.orgel.2014.07.037>.

References

- [1] (a) T.J. Scheffer, J. Nehring, A new, highly multiplexable liquid crystal display, *Appl. Phys. Lett.* 45 (1984) 1021–1022; (b) H.K. Bisoyi, S. Kumar, Liquid-crystal nanoscience: an emerging avenue of soft self-assembly, *Chem. Soc. Rev.* 40 (2011) 306–319; (c) M. Gonidec, F. Luis, A. Vichez, J. Esquena, D.B. Amabilino, J. Veciana, A liquid-crystalline single-molecule magnet with variable magnetic properties, *Angew. Chem. Int. Ed.* 49 (2010) 1623–1626; (d) S.J. Woltman, G.D. Jay, G.P. Crawford, Liquid-crystal materials find a new order in biomedical applications, *Nat. Mater.* 6 (2007) 929–938.
- [2] (a) B.R. Kaafarani, Discotic liquid crystals for opto-electronic applications, *Chem. Mater.* 23 (2011) 378–396; (b) S. Sergeev, W. Pisula, Y.H. Geerts, Discotic liquid crystals: a new generation of organic semiconductors, *Chem. Soc. Rev.* 36 (2007) 1902–1929; (c) Y. Shimizu, K. Oikawa, K. Nakayama, D. Guillon, Mesophase semiconductors in field effect transistors, *J. Mater. Chem.* 17 (2007) 4223–4229; (d) H. Iino, J. Hanna, Ambipolar charge carrier transport in liquid crystals, *Opto-Electron. Rev.* 13 (2005) 295–302; (e) M. O'Neill, S.M. Kelly, Liquid crystals for charge transport, luminescence, and photonics, *Adv. Mater.* 5 (2003) 1135–1146.
- [3] (a) K. Ohta, K. Hatsusaka, M. Sugibayashi, M. Ariyoshi, K. Ban, F. Maeda, R. Naito, K. Nishizawa, A.M. van de Craats, J.M. Warman, Discotic liquid crystalline semiconductors, *Mol. Cryst. Liq. Cryst.* 397 (2003) 25–45; (b) S. Sergeev, E. Pouzet, O. Debever, J. Levin, J. Gierschner, J. Cornil, R. Gomez-Aspe, Y.H. Geerts, Liquid crystalline octaalkoxycarbonyl phthalocyanines: design, synthesis, electronic structure, self-aggregation and mesomorphism, *J. Mater. Chem.* 17 (2007) 1777–1784; (c) K. Ohta, L. Jacquemin, C. Sirlin, L. Bosio, J. Simon, Influence of the nature of the side chains on the mesomorphic properties of octasubstituted phthalocyanine derivatives, *New J. Chem.* 12 (1988) 751–754.
- [4] (a) M.K. Engel, P. Bassoul, L. Bosio, H. Lehmann, M. Hanack, J. Simon, Mesomorphic molecular materials. Influence of chain length on the structural properties of octa-alkyl substituted phthalocyanines, *Liq. Cryst.* 15 (1993) 709–722; (b) J. Simon, C. Sirlin, Mesomorphic molecular materials for

- electronics, opto-electronics, iono-electronics: octaalkylphthalocyanine derivatives, *Pure Appl. Chem.* 61 (1989) 1625–1629;
- (c) M.J. Cook, Properties of some alkyl substituted phthalocyanines and related macrocycles, *Chem. Rec.* 2 (2002) 225–236;
- (d) S. Laschat, A. Baro, N. Steinke, F. Giesselmann, C. Hagele, G. Scalia, R. Judele, E. Kapatsina, S. Sauer, A. Schreivogel, M. Tosoni, Discotic liquid crystals: from tailor-made synthesis to plastic electronics, *Angew. Chem. Int. Ed.* 46 (2007) 4832–4887.
- [5] C. Piechocki, J. Simon, A. Skoulios, D. Guillon, P. Weber, Discotic mesophases obtained from substituted metallophthalocyanines. toward liquid crystalline one-dimensional conductors, *J. Am. Chem. Soc.* 104 (1982) 5245–5247.
- [6] (a) S. Tuncel, E.N. Kaya, M. Durmuş, T. Basova, A.G. Gürek, V. Ahsen, H. Banimuslem, A. Hassand, Distribution of single-walled carbon nanotubes in pyrene containing liquid crystalline asymmetric zinc phthalocyanine matrix, *Dalton Trans.* 43 (2014) 4689–4699;
- (b) N.B. Chaure, C. Pal, S. Barard, T. Kreouzis, A.K. Ray, A.N. Cammidge, I. Chambrier, M.J. Cook, C.E. Murphy, M.G. Cain, A liquid crystalline copper phthalocyanine derivative for high performance, organic thin film transistors, *J. Mater. Chem.* 22 (2012) 19179–19189;
- (c) C.H. Lee, Y.-W. Kwon, D.H. Choi, Y.H. Geerts, E. Koh, J. Jin, High-temperature ferromagnetism of a discotic liquid crystal dilutely intercalated with iron(III) phthalocyanine, *Adv. Mater.* 22 (2010) 4405–4409.
- [7] (a) K. Ban, K. Nishizawa, K. Ohta, A.M. van de Craats, J.M. Warman, I. Yamamoto, H. Shirai, Discotic liquid crystals of transition metal complexes 29: mesomorphism and charge transport properties of alkylthio-substituted phthalocyanine rare-earth metal sandwich complexes, *J. Mater. Chem.* 11 (2001) 321–331;
- (b) F. Nekelson, H. Monobe, M. Shiroc, Y. Shimizu, Liquid crystalline and charge transport properties of double-decker cerium phthalocyanine complexes, *J. Mater. Chem.* 17 (2007) 2607–2615;
- (c) R. Natio, K. Ohta, H. Shirai, Discotic liquid crystals of transition metal complexes: 28. Temperature-dependent electronic spectra and X-ray structural analysis of discotic liquid crystalline bis(octakisdodecyloxyphthalocyaninato)lutetium(III) complex, *J. Porphyrins Phthalocyanines* 5 (2001) 44–50.
- [8] (a) Y. Zhang, W. Jiang, J. Jiang, Q. Xue, Synthesis and liquid crystal behavior of tris[2,3,9,10,16,17,23,24-octakis(octylxy) phthalocyaninato] rare earth complexes, *J. Porphyrins Phthalocyanines* 11 (2007) 100–108;
- (b) Y. Zhang, J. Jiang, X. Sun, Q. Xue, Liquid crystal behaviour of 2,3,9,10,16,17,23,24-octakis(octylxy)phthalocyanine-containing gadolinium sandwich complexes, *Aust. J. Chem.* 62 (2009) 455–463.
- [9] (a) H. Wang, K. Qian, K. Wang, Y. Bian, J. Jiang, S. Gao, Sandwich-type tetrakis(phthalocyaninato) dysprosium–cadmium quadruple-decker SMM, *Chem. Commun.* 47 (2011) 9624–9626;
- (b) H. Wang, T. Liu, K. Wang, C. Duan, J. Jiang, Tetrakis(phthalocyaninato) rare-earth-cadmium-rare-earth quadruple-decker sandwich SMMs: suppression of QTM by long-distance f–f interactions, *Chem. Eur. J.* 18 (2012) 7691–7694;
- (c) H. Shang, H. Wang, K. Wang, J. Kan, W. Cao, J. Jiang, Sandwich-type tetrakis(phthalocyaninato) rare earth(III)–cadmium(II) quadruple-deckers. The effect of f–electrons, *Dalton Trans.* 42 (2013) 1109–1115.
- [10] (a) B. Dong, T. Sakurai, Y. Bando, S. Seki, K. Takaishi, M. Uchiyama, A. Muranaka, H. Maeda, Ion-based materials derived from positively and negatively charged chloride complexes of π -conjugated molecules, *J. Am. Chem. Soc.* 135 (2013) 14797–14805;
- (b) Y. Haketa, Y. Honsho, S. Seki, H. Maeda, Ion materials comprising planar charged species, *Chem. Eur. J.* 18 (2012) 7016–7020;
- (c) B. Dong, T. Sakurai, Y. Honsho, S. Seki, H. Maeda, Cation modules as building blocks forming supramolecular assemblies with planar receptor–anion complexes, *J. Am. Chem. Soc.* 135 (2013) 1284–1287.
- [11] R. Wang, R. Li, Y. Bian, C.-F. Choi, D.K.P. Ng, J. Dou, D. Wang, P. Zhu, C. Ma, R.D. Hartnell, D.P. Arnold, J. Jiang, Studies of “Pinwheel-Like” bis[1,8,15,22-tetrakis(3-pentyloxy)phthalocyaninato] rare earth(III) double-decker complexes, *Chem. Eur. J.* 11 (2005) 7351–7357.
- [12] P. Gans, J.-C. Marchon, C.A. Reed, One-electron oxidation of chloroiron(III) tetraphenylporphyrin cation radical in the oxidized product, *Nouveau. J. De. Chemie.* 5 (1981) 203–204.
- [13] T. Fukuda, K. Hata, N. Ishikawa, Observation of exceptionally low-lying π – π^* excited states in oxidized forms of quadruple-decker phthalocyanine complexes, *J. Am. Chem. Soc.* 134 (2012) 14698–14701.
- [14] (a) X. Li, D. Qi, C. Chen, L. Yang, J. Sun, H. Wang, X. Li, Y. Bian, Bis[octakis(2,6-dimethylphenoxy)phthalocyaninato] rare earth(III) complexes: structure, spectroscopic, and electrochemical properties, *Dyes Pigments* 101 (2014) 179–185;
- (b) Y. Zhang, X. Cai, P. Yao, H. Xu, Y. Bian, J. Jiang, Location of the hole and acid proton in neutral nonprotonated and protonated mixed (phthalocyaninato)(porphyrinato) Yttrium double-decker complexes: density functional theory calculations, *Chem. Eur. J.* 13 (2007) 9503–9514;
- (c) N. Sheng, R. Li, C.-F. Choi, W. Su, D.K.P. Ng, X. Cui, K. Yoshida, Nagao Kobayashi, J. Jiang, Heteroleptic bis(Phthalocyaninato) europium(III) complexes fused with different numbers of 15-Crown-5 moieties. Synthesis, spectroscopy, electrochemistry, and supramolecular structure, *Inorg. Chem.* 45 (2006) 3794–3802.
- [15] M. Kasha, H. Rawls, M.A. El-Bayoumi, The exciton model in molecular spectroscopy, *Pure Appl. Chem.* 11 (1965) 371–392.
- [16] (a) A. Bromby, W. Kan, T. Sutherland, Liquid crystalline 21,23-dithiaporphyrins, *J. Mater. Chem.* 22 (2012) 20611–20617;
- (b) T. Sakurai, K. Tashiro, Y. Honsho, A. Saeki, S. Seki, A. Osuka, A. Muranaka, M. Uchiyama, J. Kim, S. Ha, K. Kato, M. Takata, T. Aida, Electron- or hole-transporting nature selected by side-chain-directed π -stacking geometry: liquid crystalline fused metalloporphyrin dimers, *J. Am. Chem. Soc.* 133 (2011) 6537–6540;
- (c) T. Sakurai, K. Shi, H. Sato, K. Tashiro, A. Osuka, A. Saeki, S. Seki, S. Tagawa, S. Sasaki, H. Masunaga, K. Osuka, M. Takata, T. Aida, Prominent electron transport property observed for triply fused metalloporphyrin dimer: directed columnar liquid crystalline assembly by amphiphilic molecular design, *J. Am. Chem. Soc.* 130 (2008) 13812–13813.
- [17] Y. Zhang, N. Pan, Q. Xue, M. Bai, J. Jiang, Synthesis and liquid crystal behavior of bis[3,4,12,13,21,22,30,31-octa(dodecylthio)-2,3-naphthalocyaninato] rare earth complexes, *J. Porphyrins Phthalocyanines* 10 (2006) 1132–1139.
- [18] Y. Chen, M. Bouvet, T. Sizun, Y. Gao, C. Plassard, E. Lesniewska, J. Jiang, Facile approaches to build ordered amphiphilic tris(phthalocyaninato) europium triple-decker complex thin films and their comparative performances in ozone sensing, *Phys. Chem. Chem. Phys.* 12 (2010) 12851–12861.
- [19] D. Atilla, N. Kiliç, Fatma Yuksel, Z.Z. Öztürk, V. Ahsen, Synthesis, characterization, mesomorphic and electrical properties of tetrakis(alkylthio)-substituted lutetium(III) bisphthalocyanines, *Synth. Met.* 159 (2009) 13–21.
- [20] R.D. Gould, Structure and electrical conduction properties of phthalocyanine thin films, *Coord. Chem. Rev.* 156 (1996) 237–274.